Femtosecond Studies of Electronic Relaxation, Vibrational Relaxation, and Rotational Diffusion in all-*trans*-1,8-Diphenyl-1,3,5,7-octatetraene

W. Atom Yee*

Department of Chemistry, Santa Clara University, Santa Clara, California 95053

Robert H. O'Neil,† James W. Lewis, Jin Z. Zhang,* and David S. Kliger*

Department of Chemistry and Biochemistry, University of California, Santa Cruz, California 95064

Received: September 30, 1998; In Final Form: January 4, 1999

Femtosecond transient absorption studies of the excited singlet state dynamics of all-*trans*-1,8-diphenyl-1,3,5,7-octatetraene were conducted in various hydrocarbon solvents at room temperature using 390 nm excitation and probe wavelengths between 630 and 820 nm. Linear dichroism measurements show that one of the decay components (100−150 ps) arises from rotational diffusion. The solvent viscosity dependence is consistent with that interpretation. Transient absorptions of the S_2 ($1B_u$) and S_1 ($2A_g$) states show ultrafast $S_2 \rightarrow S_1$ internal conversion (470−600 fs) in association with possible vibrational relaxation within S_1 and S_2 on similar time scales.

I. Introduction

The all-*trans*-α,ω-diphenylpolyenes serve as models for the polyene chromophore of visual pigments, carotenoids, and other biological systems of interest, and their photochemical and photophysical properties have been studied extensively.[1] In 1972 in seminal companion papers, Hudson and Kohler[2] first reported experimental evidence of a low lying forbidden 2^1A_g state below the one-photon allowed 1^1B_u state in all-*trans*-1,8-diphenyl-1,3,5,7-octatetraene (DPO), and Schulten and Karplus[3] demonstrated that inclusion of doubly excited configurations in calculations of polyene electronic structure leads to lowering of A_g excited singlet state energies and that this result might be general for all polyenes and related compounds. Subsequently, it has been established that the lowest excited singlet state of diphenylpolyenes is the forbidden $2A_g$ state for chain lengths of three double bonds (1,6-diphenyl-1,3,5-hexatriene, DPH) or greater. For 1,4-diphenyl-1,3-butadiene (DPB), the two excited state levels are nearly degenerate. In the gas phase, the S_1 state of DPB is the $2A_g$ state,[4,5] but the order is reversed in the condensed phase because molecule−solvent interactions preferentially stabilize the $1B_u$ state.[6,7]

To characterize the nature of diphenylpolyene excited states and to study their dynamics, transient (excited state) absorption spectroscopy has been employed extensively. In this paper, we report femtosecond transient absorption studies of DPO. For background, we briefly review some of the earlier transient absorption studies on diphenylpolyenes. The nanosecond absorption spectra of DPB, DPH, and DPO were reported by Chattopadhyay and Das[8] and by Goldbeck et al.[7] In the former work, a strong absorption band near 450 nm was observed in the spectra of all three compounds. For DPH and DPO, the bands were interpreted as S_1 absorption from the lowest lying excited A_g state to an upper excited B_u state, based on previous assignments from one- and two-photon absorption spectroscopic studies. Also, DPH and DPO spectra exhibited weaker absorption at longer (550−700 nm) wavelengths. In the latter work, DPO and DPH spectra showed two distinct peaks, at ∼450 and ∼650 nm. The experimental spectra were compared to S_1 spectra calculated for both A_g and B_u excited states, and good agreement was found for the assignment of the S_1 state as an A_g state. The spectrum of DPB showed only one peak at ∼650 nm, and the S_1 state was assigned as a B_u state. The DPB assignment was supported in a following study of 1,5-diphenyl-2,3,4,6,7,8-hexahydronaphthalene,[9] a DPB analogue compound.

The picosecond time domain excited singlet state absorption spectra of DPB,[10] and of DPH and DPO,[11] were first reported by Rulliere and co-workers. These spectra agreed qualitatively with the lower resolution nanosecond spectra obtained by Goldbeck et al. However, their time-resolved studies showed that spectra were generally time dependent, with intensities of absorption features at longer wavelengths growing in time relative to shorter wavelengths. In DPB, a shoulder on the red edge of the 650 nm $1B_u$ absorption band was observed at 100 ps following excitation, and this shoulder was assigned to absorption by the $2A_g$ state. In DPH and DPO, the 650 nm absorption band appeared to grow in relation to the 450 nm band with postexcitation time. Similarly to DPB, the time-dependent spectra of DPH and DPO were interpreted by reassigning the 450 and 650 nm bands in DPH and DPO spectra to absorption by two different excited states, the $1B_u$ and $2A_g$ states, respectively. The time dependence of absorption was explained in terms of conformational changes involving large amplitude phenyl−vinyl twisting motions in the excited state. At lower temperatures, the greater relative increase of 650 nm absorption was attributed to hindrance of conformational changes by solvent and to thermal equilibrium favoring more population of the lower A_g excited state.

Later, transient absorption measurements by Wallace-Williams et al.[12] on DPB and several related compounds using femtosecond and picosecond time resolution showed no time

† Current address: Department of Biochemistry and Biophysics, Macromolecular Structure Group, University of California, San Francisco, CA 94143.

* To whom correspondence should be addressed.

10.1021/jp983922l CCC: $18.00
Published on Web 02/13/1999

dependence of the transient absorption of DPB on the picosecond time scale as earlier reported. Additionally, Hilinski et al.[13] studied the temporal behavior of the excited singlet state absorption and fluorescence of DPH in methylcyclohexane in the picosecond time domain. Their raw absorption spectra reproduced the earlier reported spectral time dependence. However, when the spectra were corrected for wavelength variation of the speed of light in the continuum probe pulse (chirp effect), the time dependence of the excited-state spectrum disappeared. It was concluded that the entire transient absorption spectrum of DPH in methylcyclohexane should be assigned to absorption by the $2A_g$ state.

Although no spectral evidence for excited state conformational changes in the diphenylpolyenes is detectable in the nanosecond and picosecond time domains, such relaxation processes might be observed with faster time resolution. Studies on phenyl twisting in triphenylmethane dyes[14] indicate that large amplitude phenyl torsion takes place on the time scale of a few picoseconds in the viscosity range of common solvents, so we expect this motion to be easily observed with our 100 fs time resolution. Recently, we reported preliminary femtosecond measurements[15] on DPB, diphenylcyclopentadiene (DPCP, a DPB analogue), DPH, and DPO in cyclohexane at room temperature using 390 nm excitation and probe wavelengths of 720 and 780 nm. Fast decay components observed in DPH and DPO were attributed to absorption by initially excited S_2 with decay rates of ~450−600 fs assigned to $S_2 \rightarrow S_1$ internal conversion processes, in accordance with the Hudson−Kohler model. No fast decay components were observed for DPB and DPCP, which are initially excited to S_1. In this paper, we report additional femtosecond results for DPO showing rotational diffusion and vibrational relaxation processes.

II. Experimental Section

Materials. DPO (Aldrich) was purified by recrystallization from ethanol. All solvents were spectroscopic grade and received no further purification.

Transient Absorption Measurements. Samples were prepared with absorbance of ~1.5 at 390 nm in 1-cm path length quartz cells and then deoxygenated by bubbling with dry nitrogen for 5 min. All experiments were performed in static solution in stoppered cells at room temperature.

The pump−probe apparatus used for the transient absorption measurements is based on a Ti:sapphire laser system described in detail elsewhere.[16] Seed pulses for the regenerative amplifier with a 40 fs duration and an energy of 2 nJ/pulse were provided by a home-built Ti:sapphire oscillator running at a repetition rate of 90 MHz. The oscillator was pumped by a Coherent CW argon-ion laser with a power of 4.0 W. The seed pulses provided the timing for the regenerative amplifier running at 1 kHz using a divider circuit driven by a 1 ns response photodiode monitoring the oscillator output. The 40 fs seed pulses were temporally stretched to approximately 200 ps by a Quantronix model 4820 pulse stretcher/compressor and then injected into a Quantronix model 4800 Ti:sapphire regenerative amplifier pumped by a 1 kHz Q-switched, intercavity-doubled Nd:YLF laser (Quantronix model 527), which produced 5 W of 527 nm light. The amplified pulses were then recompressed in the Quantronix stretcher/compressor to approximately 150 fs, with a final energy of 200 mJ centered at 780 nm with a bandwidth of 30 nm fwhm. The amplified output was then focused onto a 1 mm KDP crystal to produce the doubled 390 nm pump beam with ~150 fs pulses with energy of 30 μJ/pulse. The beam containing both the fundamental (probe) and the doubled (pump) beams was then recollimated, and the fundamental and doubled beam was split using a dichroic mirror designed to reflect 390 nm and to pass 780 nm light. The probe beam was then delayed in time relative to the pump beam by using an optical delay line consisting of a computer-controlled translation stage (Newport/Klinger UT100.150PP) having a 1 μm resolution producing a maximum delay of 1.0 ns. Before being directed onto the sample, the polarization of the pump beam was controlled using a zero-order half-wave plate (CVI Laser Corp.) as a polarization rotator, which allows change of the relative polarization of the pump beam with respect to the probe beam. The remaining fundamental at 780 nm was focused into a 1-cm quartz flat to produce a white light continuum from 400 to 900 nm. This beam was then recollimated before having the probe wavelength selected by a 10 nm fwhm interference band-pass filter.

For the linear dichroism measurements, the vertically polarized component was selected by passing the beam through a Glan−Thompson polarizer (CVI Laser Corp.). Without this polarizer, the polarization of the continuum light was variable and depended strongly on the exact position of the focus within the quartz plate. The probe beam was split into a signal and reference beam to allow pulse-to-pulse fluctuations to be eliminated by normalizing each pulse. Using a 10-cm focal length lens, the pump and probe beams were focused and overlapped in a 0.5 mm spot slightly before the beam focus in the sample cuvette. The signal and reference beams were detected by two large area photodiodes (1 cm^2, Hamamatsu S3509-3) with any nonabsorbed pump beam being removed with a slit at the signal detector and filters to reject 390 nm light. The output of the signal and reference diodes were processed by a computer that controlled a dual channel gated integrator working in conjunction with an 11 bit ADC (LeCroy 4301) installed in a DSP 860 CAMAC crate. Typically, 5000 laser pulses were averaged for each data point. The pump and probe powers were adjusted using neutral density filters, and tests were performed to be sure no signal from multiphoton ionization of the solvent occurred. Sample degradation was monitored by routinely taking ground-state absorbance measurements.

III. Results and Discussion

Absorption Spectra of S_0 and S_1. The ground-state absorption spectrum of DPO in cyclohexane solution is shown in Figure 1 and is identical to the spectrum obtained by Zechmeister[17] for the all-trans isomer. It is presented here to assist with description of our experimental results. The 390 nm excitation wavelength indicated in the figure lies very near the 0−0 vibronic peak of the strong $1B_u \leftarrow 1A_g$ absorption band. Weak but significant absorption bands near 240 and 270 nm are discussed below.

Figure 2 shows the nanosecond S_1 absorption spectrum of DPO in cyclohexane. It exhibits two bands with maxima at about 460 and 650 nm, in agreement with the earlier low-resolution spectrum obtained in the range 420−780 nm by Goldbeck et al.[7] Figure 3 shows energy levels associated with the ground- and excited-state spectra of Figures 1 and 2, respectively. Because the S_1 and S_0 electronic states are both of A_g symmetry, their absorption spectra follow the same selection rules, namely absorptive transitions to states of B_u symmetry are allowed. Therefore, both spectra contain transitions that have different initial states but the same final states. The $1B_u$ and $2A_g$ energies are obtained directly from ground-state absorption and fluorescence emission spectra, respectively. The 460 nm band in the S_1 spectrum involves the same final state ($8B_u$) as the weak band located at 240 nm in the S_0 spectrum, and the 650 nm

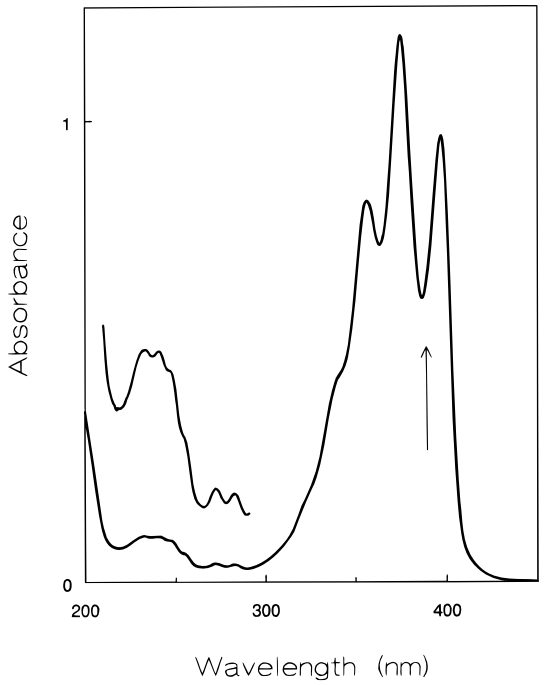

Figure 1. Ground-state absorption spectrum of DPO in cyclohexane. The arrow indicates the 390 nm excitation wavelength for femtosecond transient absorption measurements.

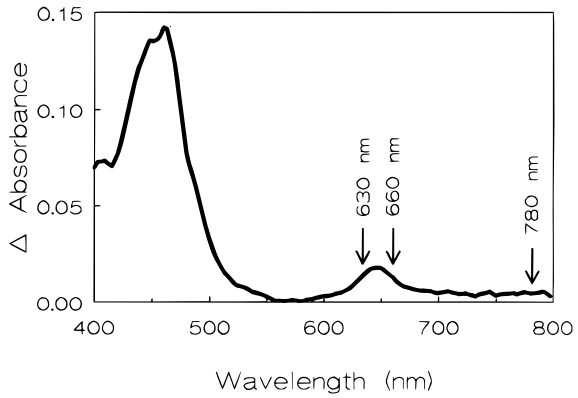

Figure 2. Nanosecond $S_n \leftarrow S_1$ transient absorption spectrum of DPO in cyclohexane at room temperature obtained with 355 nm excitation and 5 ns gate. Arrows indicate the probe wavelengths used in femtosecond decay measurements.

band involves the same final state ($5B_u$) as the weak band at 270 nm.[7] The relative intensities of the two bands in the nanosecond S_1 spectrum are approximately the same as in the S_0 spectrum, as might be expected even though Franck−Condon factors should be somewhat different between transitions originating from S_1 and S_0.

Femtosecond Pump−Probe Experiments. Femtosecond pump−probe experiments were conducted at three different monitoring wavelengths (see Figure 2). Two probe wavelengths, 630 and 660 nm, are on either side of the band maximum (∼650 nm) observed in the nanosecond S_1 spectrum. The nanosecond spectrum in the region of the 780 nm probe wavelength is relatively low and flat, showing no discernible absorption band. This wavelength is near the $S_n \leftarrow S_2$ transition predicted by theoretical calculations for DPO.[7]

Figure 4 shows normalized femtosecond transient absorption results in cyclohexane on a time scale out to 600 ps with nominally parallel pump and probe polarizations. It can be seen that nearly instantaneous absorption (instrument limited rise, <100 fs) occurs at all three probe wavelengths. These data show

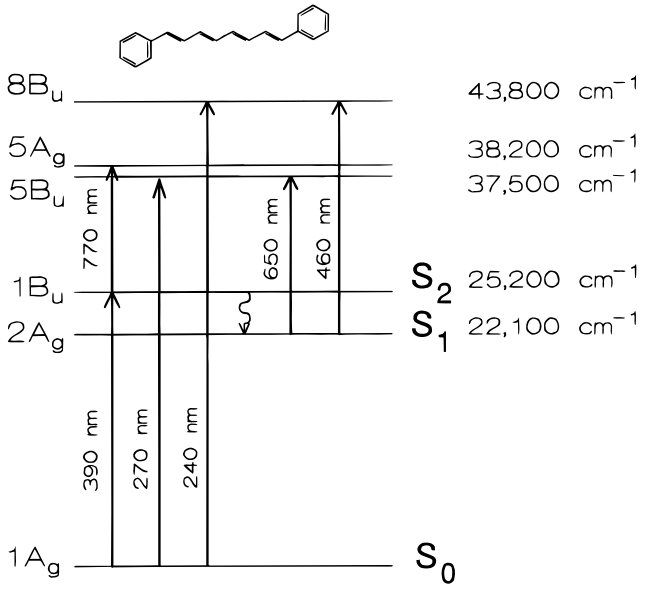

Figure 3. DPO electronic energy levels showing absorptive transitions from S_0, S_1, and S_2 states. Energies (cm^{-1}) are determined from spectra. Assignments involving the $5B_u$, $5A_g$, and $8B_u$ states are based on ref 7.

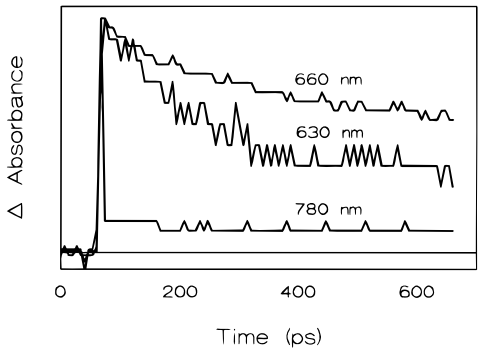

Figure 4. Normalized unpolarized transient differential absorption versus time for DPO measured at 630, 660, and 780 nm. Decays at 630 and 660 nm are due to rotational diffusion. At 780 nm, the strong absorption with very fast decay is attributed to absorption by the initially excited S_2 state.

no indication of temporal evolution of the 650 nm excited-state absorption band in terms of increasing absorption intensity on the picosecond time scale as described above. Because the S_1 lifetime is 6.5 ns,[18] on the time scale of Figure 4 almost no electronic relaxation of S_1 takes place, and the signal would be expected to be nearly flat following initial excitation. At both 630 and 660 nm, decay components of ∼100 ps are present that are therefore too fast to be assigned to electronic relaxation to S_0. At 780 nm, there are two distinct components: one, a decay on a femtosecond time scale, and a second decay that is so slow as to appear essentially flat.

Rotational Diffusion. A possible explanation for the ∼100 ps decay components seen in Figure 4 is rotational diffusion. This could occur because there is inherent polarization in our pump−probe method that produces anisotropic transient absorption. It should be noted that even an unpolarized probe beam can detect absorbance changes due to molecular rotation. To test this possibility, linear dichroism experiments were performed in three solvents of different viscosities. The upper panel of Figure 5 shows results using parallel and perpendicular orientations of the pump and probe beams in cyclohexane solvent. The lower panel shows linear dichroism ($\Delta A_{\parallel} - \Delta A_{\perp}$) of DPO versus time, which is well fit to an exponential decay

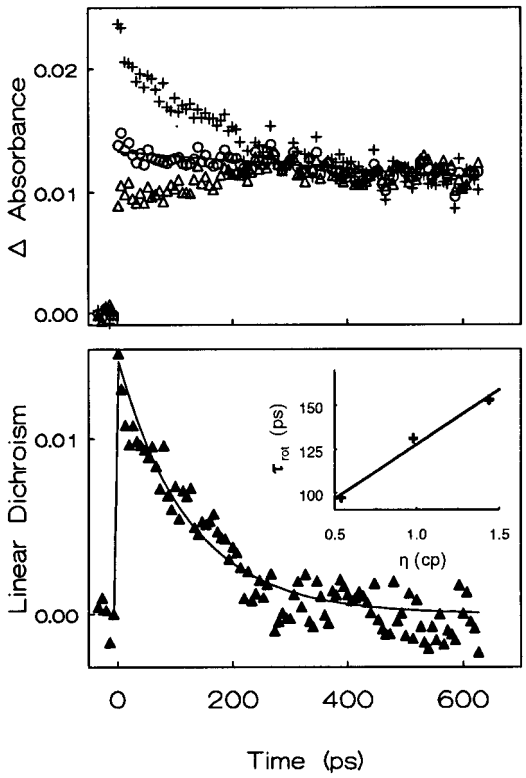

Figure 5. (upper panel) Transient differential absorption at 660 nm in cyclohexane versus time, using parallel (+) and perpendicular (Δ) orientations of pump and probe beams. Also shown is the average $\Delta A = (\Delta A_{\parallel} + 2\Delta A_{\perp})/3$ (○). (lower panel) Linear dichroism (LD = $\Delta A_{\parallel} - \Delta A_{\perp}$) versus time for data shown in the upper panel. The exponential fit of 131 ps is the rotational diffusion lifetime. Inset shows rotational diffusion lifetimes versus solvent viscosity for octane, cyclohexane, and dodecane.

of 131 ps. Similar good fits were obtained in octane and dodecane. The inset of the lower panel shows that the DPO linear dichroism lifetimes increase with an increase in viscosity, as expected for a rotational diffusion process.[19]

The values obtained for DPO rotational diffusion times may be compared to what has been determined for this process in two other systems. Using picosecond polarized transient bleaching, Quitevis and Horng[19] measured ground-state rotational diffusion times of merocyanine 540 in numerous solvents, and they found a good linear relationship between rotational diffusion times and solvent viscosity. For a solvent viscosity of 1 cP, a rotational diffusion time of ∼220 ps is expected. The DPO value of 131 ps at this same viscosity is in the right order of magnitude for a rotational diffusion process, and the merocyanine 540 value is expected to be higher because it has a larger hydrodynamic radius than DPO. Using differential polarized phase fluorometry, Lakowicz[20] measured rotational diffusion times of ∼4.5 ns for DPH in propylene glycol solvent, whose viscosity is ∼45 cP at 20 °C.[21] This means that the rotational diffusion time for DPH should be near 100 ps at a viscosity of 1 cP. The DPH value is expected to be lower than what is measured for DPO because DPH has a smaller hydrodynamic radius than DPO.

We note that our plot of rotational diffusion time vs solvent viscosity, shown in the inset of Figure 5, does not extrapolate to the graph origin. This may be due to two factors: simple experimental uncertainty and the possibility of multiexponential decay of the linear dichroism. The latter effect is based on the fact that the DPO electronic transition dipole moment is not oriented along the major axis of the polyene chain. Hudson and

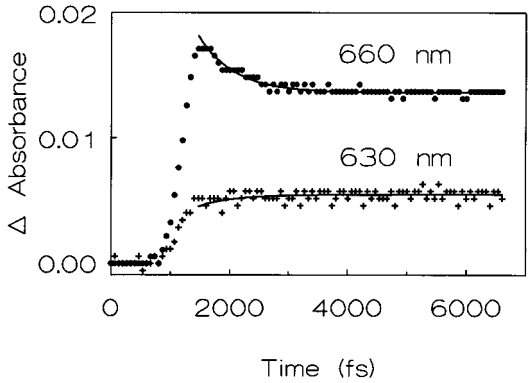

Figure 6. Transient differential absorption versus time for DPO in cyclohexane measured at 630 and 660 nm. Data are fit to a single-exponential decay with a time constant of 600 fs, plus an offset. No deconvolution is performed to account for the instrumental response.

Birge[22] have shown recently that this is a general property of all polyenes and is retained in the infinite chain limit. The off-axis angle (∼13−15°) would produce another (very fast) decay component in the DPO linear dichroism measurements. The rotational lifetimes shown in Figure 5 are obtained from single-exponential fitting because our data do not justify additional components.

650 nm Absorption Band Relaxation. Figure 6 shows results for the 630 and 660 nm measurements on a shorter time scale. At early times, different temporal behavior can be clearly seen. In the 660 nm data, fast absorption is followed by sub-picoseond decay, whereas in this same time region at 630 nm, there is growing in of absorption. A possible explanation of such behavior is that besides the known absorbance by S_1 in this region, S_2 coincidentally has a band somewhat red-shifted relative to the 650 nm absorbance originating from S_1. This explanation has the advantage of being consistent with the pulse-width-limited rise seen for the 660 nm absorbance. The implied attribution of the ∼600 fs relaxation to $S_2 \rightarrow S_1$ radiationless conversion with vibrational relaxation being more rapid is also consistent with behavior of the 780 nm band associated primarily with absorbance by S_2 (see below).

Alternatively, the behavior seen in Figure 6 could arise from vibrational relaxation in S_1. Following excitation of the DPO populating the S_2 state, if $S_2 \rightarrow S_1$ radiationless conversion is rapid, then vibrationally excited S_1 would result. The absorption spectrum would thus be initially red-shifted and then undergo a blue shift with time. Because the 660 nm probe wavelength lies on the red edge of the band maximum, absorption would increase and then decrease as the band maximum moves through this wavelength. Data shown in the figure are well fit by a relaxation time of ∼600 fs, which is in the range expected for vibrational relaxation.

Solvent Dependence of S_2 Absorption. Figure 7 (reproduced from ref 15) shows data for measurements at 780 nm in three hydrocarbon solvents: cyclohexane, dodecane, and octane. Strong transient absorption at this wavelength arises from initially excited S_2, and corresponds to the $5A_g \leftarrow 2B_u$ transition. A small solvent dependence is noticeable in the data. Cyclohexane and dodecane exhibit similar behavior, giving S_2 decay times of 570 and 600 fs (±10%), respectively, while the decay time in octane is 470 fs. Because cyclohexane and dodecane have similar refractive indexes, and therefore similar polarizabilities, and because the $1B_u-2A_g$ energy gap is a function of solvent polarizability,[23] similar S_2 decay rates are expected on the basis of the energy gap law of radiationless transitions.

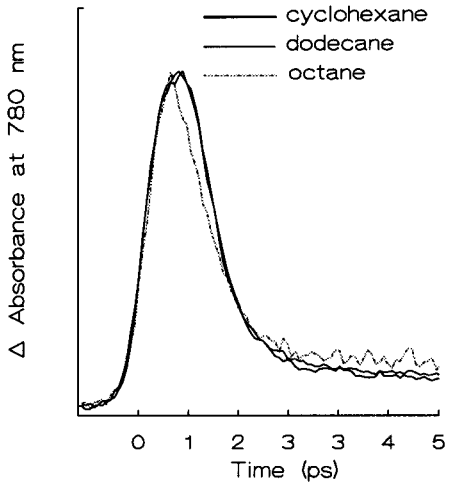

Figure 7. Transient differential absorption versus time for DPO measured at 780 nm in cyclohexane, dodecane, and octane solvents at room temperature. Data are scaled to the same maximum intensity. Time constants (±10%) for the fast decay components were determined to be 570, 600, and 470 fs, respectively.

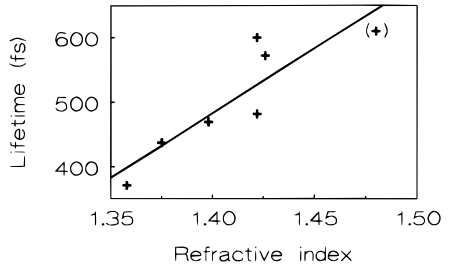

Figure 8. Decay times for DPO fast decay components measured at 780 nm versus refractive index for a range of hydrocarbon solvents. Decay times were obtained as single-exponential fits deconvolved with a Gaussian instrument function. The value for benzene (shown in parentheses), has a larger uncertainty than the others.

However, the energy gap is larger in octane so that a slower S_2 decay would be expected, and the opposite is observed.

Figure 8 shows S_2 decay rates measured at 780 nm as a function of solvent refractive index. Although the refractive index range is limited (pentane lowest to benzene highest), it is clear that the trend is for increasing (slower) S_2 decay times as the S_2-S_1 energy gap decreases. This behavior is perhaps not surprising since the energy gap law is based on a continuum model[24] in which the energy difference between zero-point energy levels is much greater than that which occurs in DPO (the S_2-S_1 energy gap in azulene is approximately 14000 cm^{-1}, while in DPO it is approximately 3000−3200 cm^{-1}). Instead of a continuum model, internal conversion in DPO may be optimized for specific S_2-S_1 energy gaps, which improve resonance of vibrational levels in S_1 with $v = 0$ of S_2.

Alternatively, the S_2 radiationless decay rates may depend on resonance interaction of DPO with solvent vibrational levels. For example, Schmidt and co-workers[25] have studied the collisional deactivation of singlet oxygen by solvent molecules, in which quenching occurs by energy transfer to peripheral bonds X−Y (O−H, C−H, etc.) of the solvent molecules. They found an empirical linear correlation of ln k_{XY} with the energy $E_{XY,1}$ of the highest energy fundamental vibration of X−Y peripheral bonds. In the case of oxygen, the electronic energy gap is fixed as the solvent vibrational energies are varied. For the DPO S_2 lifetime data, energies of the fundamental stretching modes of the nonaromatic hydrocarbon solvents are all about the same while the electronic energy gap is varied. Another

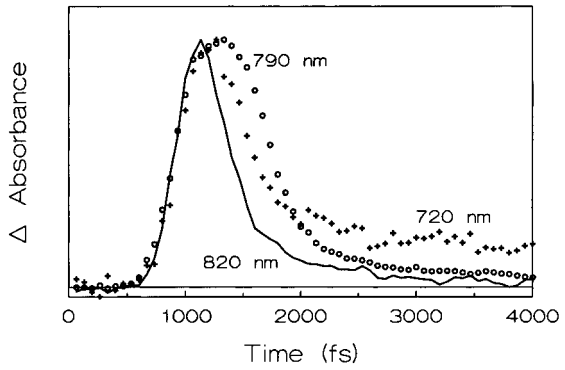

Figure 9. Transient differential absorption versus time for DPO in hexane measured at 820, 790, and 720 nm. Absorption at early times is mainly from S_2, and that at later times is from S_1.

difference is the size of the energy gap, which is much smaller in DPO (~3000 cm^{-1}) than in O_2 (~8000 cm^{-1}). Thus, for DPO, the gap is very close to resonance with 3000 cm^{-1} C−H stretch vibrations of hydrocarbon solvents.

The nonenergy gap law behavior for DPO differs from results of recent fluorescence measurements in a series of carotenes. Carotenoids have molecular and electronic structure similar to the diphenylpolyenes, especially the presence of a forbidden A_g state below the allowed B_u state. Andersson et al.[26] found a good linear dependence between the $S_2 \rightarrow S_1$ radiationless decay rate (ln k_{21}) and the S_2-S_1 energy gap for carotene analogue compounds having eight and nine double bonds (m8 and m9), where the decay rate k_{21} is determined from measured and calculated $S_2 \rightarrow S_0$ fluorescence quantum yields. However, the energy gaps reported for m8 are in the range 5200−7000 cm^{-1}. These larger gaps may account for the difference in behavior between DPO and carotenes.

Wavelength Dependence of S_2 Absorption. Normalized transient absorption data for DPO in hexane solution measured at 720, 790, and 820 nm are shown in Figure 9. While the rise of absorption occurs at similar rates at these wavelengths, there is a small but noticeable wavelength dependence of the fast decay components. This behavior is also suggestive of vibrational relaxation.[27] On the red edge of the S_2 band, vibrational relaxation would combine with $S_2 \rightarrow S_1$ radiationless conversion to accelerate the observed decay. As expected, the 820 nm data shows the fastest decay but decays at 720 and 790 nm appear to be similar. Interpretation of the rise of these signals, while apparently supportive of the model of vibrational relaxation in S_2, is complicated by the possibility that the probe pulse width may vary with wavelength. Determination of the S_2 decay rates at these wavelengths is further complicated by the fact that S_1 contributes to absorption, making analysis of the data to examine S_2 vibrational relaxation processes difficult. Figure 10 shows preliminary data for DPO in benzene solution at the same three wavelengths. It can be seen generally that decay of S_2 absorption in benzene is dramatically slower than in hexane. In addition, the benzene data show substantially more S_1 absorption at 720 and 790 nm. Of course, while discussion has been framed in terms of contrasting cases, i.e., internal conversion being either much faster or much slower than vibrational relaxation, as the complex behavior in benzene shows, the actual situation is much less clear-cut.

Our transient absorption measurements show a photophysical picture of DPO relaxation that is complex. Upon excitation of S_2, competing $S_2 \rightarrow S_1$ electronic radiationless conversion and S_2 vibrational relaxation processes occur. Similar behavior has been discerned in carotenoid systems from ultrafast fluorescence

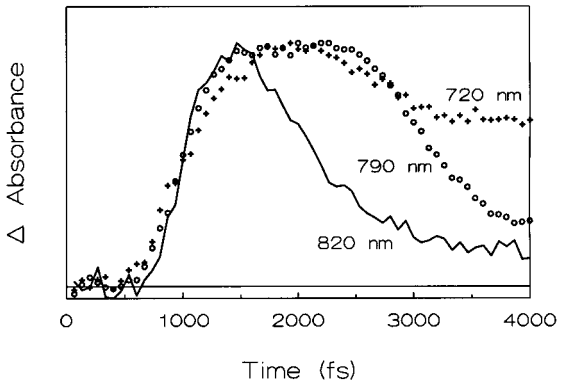

Figure 10. Transient differential absorption versus time for DPO in benzene measured at 820, 790, and 720 nm. Absorption at early times is from S_2, and that at later times is from S_1. DPO in benzene has greater S_1 absorption at 720 and 790 nm compared to hexane (see Figure 9).

measurements by Gillbro and Cogdell.[28] They observed anomalies in S_2 fluorescence excitation spectra, indicating that the rate of $1B_u \rightarrow 2A_g$ radiationless conversion is comparable to vibrational relaxation within the $1B_u$ state.

IV. Conclusions

Femtosecond transient absorption studies of DPO using 390 nm excitation and probe wavelengths from 630 to 820 nm have revealed fast photophysical processes not observed in previous nanosecond and picosecond studies. Rotational diffusion and either vibrational relaxation or decay of a nearby S_2 absorption are observed in the decay of the 650 nm band associated with DPO S_1 absorption. Decay of S_2 absorption shows a solvent dependence that does not follow an energy gap law. This may be due to quantum effects or specific solvent−solute interactions. A wavelength dependence of the S_2 decay rates indicates that S_2 vibrational relaxation may occur in competition with $S_2 \rightarrow S_1$ internal conversion. As found in earlier picosecond spectroscopic studies, no processes were observed that can be attributable to large amplitude conformational changes in DPO.

Acknowledgment. This research was supported by grants from the Petroleum Research Fund administered by the American Chemical Society (J.Z.Z.) and from the National Institutes of Health (D.S.K., Grant EY00983). We thank R. S. H. Liu, Tomas Gillbro, and William Jenks for helpful discussions and information. The authors dedicate this paper to the memory of Dr. Bryan E. Kohler.

References and Notes

(1) Hudson, B. S.; Kohler, B. E.; Schulten, K. In *Excited States*; Lim, E. C., Ed.; Academic Press: New York, 1982; Vol. 6, p 1. (b) Whitten, D. G. *Chem. Rev.* **1989**, *89*, 1691. (c) Saltiel, J.; Sun, Y.-P. In *Photochromism, Molecules, and Systems*; Durr, H., Bouas-Laurent, H., Eds.; Elsevier: Amsterdam, 1990; p 64.

(2) Hudson, B. S.; Kohler, B. E. *Chem. Phys. Lett.* **1972**, *14*, 299.

(3) Schulten, K.; Karplus, M. *Chem. Phys. Lett.* **1972**, *14*, 305.

(4) Heimbrook, L. A.; Kohler, B. E.; Spiglanin, T. A. *Proc. Natl. Acad. Sci. U.S.A.* **1983**, *80*, 4580.

(5) Shepanski, J. F.; Keelan, J. F.; Zewail, A. H. *Chem. Phys. Lett.* **1983**, *103*, 9.

(6) Velsko, S. P.; Fleming, G. R. *J. Chem. Phys.* **1982**, *76*, 3553.

(7) Goldbeck, R. A.; Twarowski, A. J.; Russell, E. L.; Rice, J. K.; Birge, R. R.; Switkes, E.; Kliger, D. S. *J. Chem. Phys.* **1982**, *77*, 3319.

(8) Chattopadhyay, S. K.; Das, P. K. *Chem. Phys. Lett.* **1982**, *87*, 145.

(9) Yee, W. A.; Horwitz, J. S.; Goldbeck, R. A.; Einterz, C. M.; Kliger, D. S. *J. Phys. Chem.* **1983**, *87*, 380.

(10) Rulliere, C.; Declemy, A.; Kottis, P. *Laser Chem.* **1985**, *5*, 185.

(11) Rulliere, C.; Declemy, A. *Chem. Phys. Lett.* **1987**, *135*, 213.

(12) Wallace-Williams, S. E.; Schwartz, B. J.; Moller, S.; Goldbeck, R. A.; Yee, W. A.; El-Bayoumi, M. A.; Kliger, D. S. *J. Phys. Chem.* **1994**, *98*, 60.

(13) Hilinski, E. F.; McGowan, W. M.; Sears, D. F.; Saltiel, J. *J. Phys. Chem.* **1996**, *100*, 3308.

(14) Ben-Amotz, D.; Harris, C. B. *J. Chem. Phys.* **1987**, *86*, 4856.

(15) Yee, W. A.; O'Neil, R. H.; Lewis, J. W.; Zhang, J. Z.; Kliger, D. S. *Chem. Phys. Lett.* **1997**, *276*, 430.

(16) Zhang, J. Z.; O'Neil, R. H.; Roberti, T. W. *J. Phys. Chem.* **1994**, *98*, 3859.

(17) Zechmeister, L.; Pinckard, J. H. *J. Am. Chem. Soc.* **1954**, *76*, 4144.

(18) Berlman, I. B. *Handbook of Fluorescence Spectra of Aromatic Molecules*, 2nd ed.; Academic Press: New York, 1971; p 323.

(19) Quitevis, E. L.; Horng, M. L. *J. Phys. Chem.* **1990,** *94*, 5684.

(20) Lakowicz, J. R. In *Time-Resolved Fluorescence Spectroscopy in Biochemistry and Biology*; Cundall, R. B., Dale, R. E., Eds.; Plenum Press: New York, 1983; p 546.

(21) *International Critical Tables;* Mc-Graw Hill: New York, 1930; Vol. VII, p 215.

(22) Birge, R. R.; Zgierski, M. Z.; Serrano-Andres, L.; Hudson, B. S. *J. Phys. Chem.* **1999**, *103*, xxx.

(23) Sklar, L. A.; Hudson, B. S.; Petersen, M.; Diamond, J. *Biochemistry* **1977**, *16*, 813.

(24) Birks, J. B. *Photophysics of Aromatic Molecules;* Wiley-Interscience: New York, 1970.

(25) Schmidt, R.; Afshari, E. *Ber. Bunsen-Ges. Phys. Chem.* **1992**, *96*, 788 and references therein.

(26) Andersson, P. O.; Bachilo, S. M.; Chen, R.-L.; Gillbro, T. *J. Phys. Chem.* **1995**, *99*, 16199.

(27) Harris, A. L.; Brown, J. K.; Harris, C. B. *Annu. Rev. Phys. Chem.* **1988**, *39*, 341.

(28) Gillbro, T.; Cogdell, R. J. *Chem. Phys. Lett.* **1989**, *158*, 312.